Direct Synthesis of Hybrid Organic−Inorganic Nanoporous Silica Microspheres. 1. Effect of Temperature and Organosilane Loading on the Nano- and Micro-Structure of Mercaptopropyl-Functionalized MSU Silica

Luc Beaudet, Kazi-Zakir Hossain, and Louis Mercier*

Department of Chemistry and Biochemistry, Laurentian University, Sudbury, Ontario, Canada P3E 2C6

Received August 21, 2002

The preparation of a series of organically functionalized wormhole-motif microspherical MSU-X silicas mesostructures was achieved by a direct synthesis process involving the addition of tetraethoxysilane (TEOS) and 3-mercaptopropyltrimethoxysilane (MPTMS) to mildly acidified solutions of a structure-directing nonionic surfactant (Igepal CA-720), followed by fluoride-mediated hydrolysis/cross-linking and surfactant extraction. The influence of organosilane content (MPTMS/TEOS ratio) and synthesis temperature on the framework order, pore structure, and particle size of the resulting mesostructures was investigated. The lattice spacings, pore volumes, and pore diameters were found to systematically increase as a function of increasing synthesis temperature. Although very poorly ordered and microporous when prepared at lower synthesis temperatures, the framework ordering and pore channel diameters of the microspheres dramatically improved when these were synthesized at temperatures above 40−45 °C. Moreover, increasing the synthesis temperature reduced the average particle sizes of the microspheres, although a sudden swelling of the particle sizes was observed in the threshold temperature zone where improved framework order and mesoporosity in the microspheres was evidenced. Incorporation of organic functional groups (MPTMS) inside the structures appeared to have little influence on the structure and morphology of the mesostructures, save for slight lattice and pore diameter contractions upon increasing organosilane group loading. By systematically varying the organosilane content and the synthesis temperature of the microspheres, functional MSU-X materials with accurately fine-tuned pore dimensions and particle diameters could therefore be obtained.

Introduction

Since the beginnings of mesostructure science a decade ago,[1] much research has been devoted to the synthesis and properties of hybrid organic−inorganic materials that possessed well-defined pore structures, highly accessible functional groups, and controlled surface reactivity.[2] These materials, which benefit from the flexibility and reactivity of tailored organic functional groups and the structural robustness and chemical inertness of the inorganic scaffold, have wide-ranging applications in many areas, including adsorption, catalysis, and high-technology fields. It is now well-established that functionalized derivatives of mesostructures can be prepared using easily implementable methods, such as grafting[3−12] or one-step synthesis[13−31] methods. Such an ever-evolving toolkit of methodologies provides the chemist with the ability to tailor materials

* To whom correspondence should be addressed. Phone: 705-675-1151, ext. 2111. Fax: 705-675-4844. E-mail: lmercier@nickel.laurentian.ca.

(1) Kresge, C. T.; Leonowicz, M. E.; Roth, W. J.; Vartuli, J. C.; Beck, J. S. *Nature* **1992**, *359*, 710.
(2) Sayari, A.; Hamoudi, S. *Chem. Mater.* **2001**, *13*, 3151.
(3) Tanev, P. T.; Chibwe, M.; Pinnavaia, T. J. *Nature* **1994**, *368*, 321.
(4) Maschmeyer, T.; Rey, F.; Sankar, G.; Thomas, J. M. *Nature* **1995**, *378*, 159.
(5) Brunel, D.; Cauvel, A.; Fajula, F.; DiRenzo, F. *Stud. Surf. Sci. Catal.* **1995**, *97*, 173.
(6) Zhang, W.; Pinnavaia, T. J. *Catal. Lett.* **1996**, *38*, 261.
(7) Zhang, W.; Wang, J.; Tanev, P. T.; Pinnavaia, T. J. *Chem. Commun.* **1996**, 979.
(8) Zhang, W.; Froba, M.; Wang, J.; Tanev, P. T.; Wong, J.; Pinnavaia, T. J. *J. Am. Chem. Soc.* **1996**, *118*, 9164.
(9) Cauvel, A.; Brunel, D.; Renzo, F. D.; Fajula, F. *AIP Conf. Proc.* **1996**, *354*, 477.
(10) Mercier, L.; Pinnavaia, T. J. *Adv. Mater.* **1997**, *9*, 500.
(11) Feng, X.; Fryxell, G. E.; Wang, L.-Q.; Kim, A. Y.; Liu, J.; Kemner, K. M. *Science* **1997**, *276*, 923.
(12) Mercier, L.; Pinnavaia, T. J. *Environ. Sci. Technol.* **1998**, *32*, 2749.
(13) Burkett, S. L.; Sims, S. D.; Mann, S. J. *J. Chem. Soc., Chem. Commun.* **1996**, 1367.
(14) Macquarrie, D. J. *Chem. Commun.* **1996**, 1961.
(15) Lim, M. H.; Blanford, C. F.; Stein, A. *J. Am. Chem. Soc.* **1997**, *119*, 4090.
(16) Fowler, C. E.; Burkett, S. L.; Mann, S. J. *Chem. Commun.* **1997**, 1769
(17) Lim, M. H.; Blanford, C. F.; Stein, A. *Chem. Mater.* **1998**, *10*, 467.
(18) Van Rhijn, W. M.; DeVos, D. E.; Sels, B. F.; Bossaert, W. D.; Jacobs, P. A. *Chem. Commun.* **1998**, 317.

10.1021/cm021294l CCC: $25.00
Published on Web 12/10/2002

that have suitable properties (both physical and chemical) for desired applications.

The incorporation of mercaptopropyltrimethoxysilane ($(MeO)_3Si(CH_2)_3SH$, MPTMS) has been widely used as a workhorse for the study of organic group functionalization in nanoporous silicas.[10−12,17−19,21,22,25−31] The interest in using this particular group essentially lies in its ability to strongly and selectively complex heavy metal ions such as mercury,[10−12,17,21,27,31] as well as to act as a precursor for sulfonic acid groups.[18,25,28] Thus, the incorporation of MPTMS into mesostructures using direct synthesis methods has proven to be most useful to prepare nanoporous materials with judiciously tailored pore structure and accurately controlled functional group loading.[17−19,21,22,25−31]

Organically functionalized derivatives of MCM-41-type mesostructures by direct synthesis have been reported, where charged surfactants are utilized as structure-directing agents.[13−18,20,22] Functionalized SBA-15 derivatives have also been reported using a similar synthetic approach in which assembly is performed using nonionic surfactants under highly acidic hydrolysis conditions.[28] Finally, neutral and nonionic surfactant assembly pathways were also used for the one-step preparation of functional HMS[14,21,23−26,29] and MSU-X[19,27,30,31] derivatives. Because nonelectrostatic assembly can be performed under neutral or near-neutral pH conditions, these mesostructures possess uncharged frameworks, allowing the complete and nondestructive removal of the porogenic surfactants by solvent extraction. In contrast, the removal of surfactant from electrostatically assembled frameworks (often synthesized under highly alkaline conditions) requires the combined use of acid leaching and solvent extraction, which may result in structural decomposition of the materials[13] or incomplete extraction of the surfactant.[15] Moreover, by avoiding the use of extreme pH conditions, the direct synthesis of functional HMS and MSU-X mesostructures may allow the incorporation of functional groups that would otherwise react or decompose in strongly acidic or strongly basic media.[19]

Recently, the synthesis of thiol-functionalized MSU-X silicas under neutral pH conditions has been shown to be most versatile for the preparation of functional mesostructures with accurately tailored pore structures and organic group composition.[30] Whereas in most types of functional mesostructures (e.g., MCM-41, HMS) the tuning of these material properties can be controlled only by adjusting the reagent stoichiometry of the synthesis mixture; MSU-X materials are unique in that temperature influences the properties of the mesostructures. A well-known property of nonionic surfactants is the temperature-dependent swelling of their hydrophobic core resulting from the coil to rod conformational changes in the ethyleneoxide (EO) segments with increasing temperature.[32] Thus, the hydrogen bonding interactions which occur between the hydrophilic EO headgroups and the silica precursors diminish as the amphiphilic character of the surfactant molecules is reduced at higher synthesis temperature. This results in the formation of mesostructures whose pore diameters systematically increase as a function of synthesis temperature, until a critical temperature (known as the cloud point) is reached where all amphilic character is lost, surfactant precipitation occurs, and no mesostructure is formed.[32] This property of nonionic surfactants was used to prepare both purely siliceous MSU-X mesostructures[32] and their functionalized derivatives[30] with pore diameters that could be accurately controlled by varying their synthesis temperatures. In addition, the thermal expansion of the hydrophobic micelle cores increases the overall hydrophobicity of the synthesis mixture, a property which was exploited to control the degree of organic group loading in the hybrid MSU-X materials.[30]

Yet another interesting aspect of MSU-X chemistry is the recent discovery that, under mildly acid conditions, the MSU-X materials adopt monodisperse micrometric spherical morphology with uniform particle sizes.[31,33,34] The ability to form mesostructures with well-defined particle shape and size represents an important but still rather underdeveloped frontier in materials science: the control of material *microstructure*. In this study, the influence of temperature and organosilane addition on the nanostructural and microstructural characteristics of mercaptopropyl-functionalized microspherical MSU-X mesostructures is investigated.

Experimental Section

Materials. All chemicals were purchased from Aldrich and used without further purification. Deionized water and 95% ethanol were used in the syntheses and extraction processes, respectively.

Mesostructure Synthesis. In a typical preparation, a mixture of tetraethoxysilane (TEOS; $(1 - X) \times 2.16 \times 10^{-2}$ mol) and 3-mercaptopropyltrimethoxysilane (MPTMS; $X \times 2.16 \times 10^{-2}$ mol) was added to 100 mL of a stirred solution of Igepal CA-720 ($C_8H_{17}-C_6H_5-(OCH_2CH_2)_{10}OH$, 3.06×10^{-2} M) which had been acidified with 5 mL of HCl 0.20 M. The mole fractions X of MPTMS with respect to the total silane (TEOS + MPTMS) used in the synthesis mixtures were 0, 0.02, 0.04, and 0.06. The mixtures were stirred for 1 h to yield clear solutions, then transferred to a water bath with a controlled temperature in the range 0−71 °C. After 30 min of thermal equilibration, NaF was added (0.03825 g). The solution was quickly stirred then left to sit undisturbed in the water bath for 24 h to allow precipitation of the product. The resulting material was then filtered and air-dried, and the framework-

(19) Richer, R.; Mercier, L. *Chem. Commun.* **1998**, 1775.
(20) Babonneau, F.; Leite, L.; Fontlupt, S. *J. Mater. Chem.* **1999**, *9*, 175.
(21) Brown, J.; Mercier, L.; Pinnavaia, T. J. *Chem. Commun.* **1999**, 69.
(22) Hall, S. R.; Fowler, C. E.; Lebeau, B.; Mann, S. *Chem. Commun.* **1999**, 201.
(23) Macquarrie, D. J.; Jackson, D. B.; Mdoe, J. E. G.; Clark, J. H. *New J. Chem.* **1999**, *23*, 539.
(24) Corriu, R. J. P.; Mehdi, A.; Reyé, C. *C. R. Acad. Sci. Ser. II C* **1999**, *2*, 35.
(25) Bossaert, W. D.; De Vos, D. E.; Van Rhijn, W. M.; Bullen, J.; Grobet, P. J.; Jacobs, P. A. *J. Catal.* **1999**, *182*, 156.
(26) Mercier, L.; Pinnavaia, T. J. *Chem. Mater.* **2000**, *12*, 188.
(27) Brown, J.; Richer, R.; Mercier, L. *Micropor. Mesopor. Mater.* **2000**, *37*, 41.
(28) Margolese, D.; Melero, J. A.; Christiansen, S. C.; Chmelka, B. F.; Stucky, G. D. *Chem. Mater.* **2000**, *12*, 2448.
(29) Mori, Y.; Pinnavaia, T. J. *Chem. Mater.* **2001**, *13*, 2173.
(30) Richer, R.; Mercier, L. *Chem. Mater.* **2001**, *13*, 2999.
(31) Bibby, A.; Mercier, L. *Chem. Mater.* **2002**, *14* (4), 1591−1597..
(32) Prouzet, E.; Pinnavaia, T. J. *Angew. Chem., Int. Ed. Eng.* **1997**, *36*, 516.
(33) Boissière, C.; van der Lee, A.; El Mansouri, A.; Larbot, A.; Prouzet, E. *Chem Commun.* **1999**, 2047.
(34) Boissière, C.; Larbot, A.; van der Lee, A.; Kooyman, P. J.; Prouzet, E. *Chem. Mater.* **2000**, *12*, 2902.

Table 1. Structural Characteristics of Pure Silica MSU-2 Microspherical Mesostructures

material designation	synthesis temp. (°C)	BET surface area ($m^2\ g^{-1}$)	mesopore volume ($cm^3\ g^{-1}$)	pore diameter (Å)	lattice spacing (Å)	wall thickness (Å)
MSU-2(MS)-0	0	774	0.35	<20	35.8	>16
MSU-2(MS)-10	10	529	0.24	<20	35.1	>15
MSU-2(MS)-15	15	761	0.34	<20	38.6	>19
MSU-2(MS)-20	20	695	0.30	<20	35.8	>16
MSU-2(MS)-25	25	800	0.36	<20	39.0	>19
MSU-2(MS)-30	30	872	0.38	<20	40.2	>20
MSU-2(MS)-35	35	884	0.41	<20	39.8	>20
MSU-2(MS)-37	37	1240	0.78	32	45.3	13
MSU-2(MS)-40	40	1193	0.84	34	47.5	14
MSU-2(MS)-43	43	1114	0.79	35	48.1	13
MSU-2(MS)-45	45	1260	0.90	35	47.0	12
MSU-2(MS)-50	50	1165	0.88	37	48.1	11
MSU-2(MS)-55	55	1110	1.00	41	50.6	10
MSU-2(MS)-61	61	1034	1.06	45	53.4	8
MSU-2(MS)-64	64	936	1.09	48	54.1	6
MSU-2(MS)-68	68	1006	1.12	49	54.9	6
MSU-2(MS)-71	71	882	1.07	51	56.5	6

Table 2. Structural Characteristics of MSU-2 Microspherical Mesostructures Prepared by Substituting 2.0 Mol % of TEOS with MPTMS

material designation	synthesis temp. (°C)	BET surface area ($m^2\ g^{-1}$)	mesopore volume ($cm^3\ g^{-1}$)	pore diameter (Å)	lattice spacing (Å)	wall thickness (Å)
MP-MSU-2(MS)-2.0-0	0	664	0.28	<20	34.8	>15
MP-MSU-2(MS)-2.0-10	10	414	0.17	<20	37.1	>17
MP-MSU-2(MS)-2.0-15	15	459	0.19	<20	36.8	>17
MP-MSU-2(MS)-2.0-20	20	505	0.22	<20	38.2	>18
MP-MSU-2(MS)-2.0-25	25	494	0.21	<20	37.8	>18
MP-MSU-2(MS)-2.0-30	30	614	0.27	<20	37.8	>18
MP-MSU-2(MS)-2.0-35	35	685	0.30	<20	37.8	>18
MP-MSU-2(MS)-2.0-37	37	994	0.47	26	45.3	19
MP-MSU-2(MS)-2.0-40	40	648	0.28	<20	40.2	>20
MP-MSU-2(MS)-2.0-45	45	1187	0.70	31	47.0	16
MP-MSU-2(MS)-2.0-50	50	1184	0.82	35	47.0	12
MP-MSU-2(MS)-2.0-55	55	1092	0.90	41	49.3	8
MP-MSU-2(MS)-2.0-61	61	1099	1.04	46	50.0	4
MP-MSU-2(MS)-2.0-64	64	991	1.04	49	51.5	3
MP-MSU-2(MS)-2.0-68	68	987	1.00	47	52.0	5
MP-MSU-2(MS)-2.0-71	71	919	1.01	51	53.5	3

bound surfactant was removed by Soxhlet extraction over ethanol for 24 h. Following the previously suggested naming system,[30] the mesostructures were hereafter designated thus: MSU-2(MS)-*T*, MP-MSU-2(MS)-2.0-*T*, MP-MSU-2(MS)-4.0-*T*, MP-MSU-2(MS)-6.0-*T*, where MP denotes the functional group (viz., mercaptopropyl), MSU-2 represents the mesostructure prototype designation (viz., mesostructures assembled using alkyl(aryl)poly(ethylene oxide) surfactants such as Igepal-CA720 are labeled as MSU-2),[35] (MS) denotes the microspherical morphology of the materials, the number denotes the percent of functional group incorporated (or 100 *X*), and *T* refers to the synthesis temperature.

Mesostructure Characterization. Powder X-ray diffraction patterns were measured on a Rigaku Rotaflex diffractometer equipped with a rotating anode and using Cu Kα radiation (Ontario Geoscience Laboratories, Sudbury, ON). The lattice spacings (*d*) of the materials were calculated by applying Bragg's Law to the maximum in the diffraction peaks observed in the patterns ($d = 1.54$ Å$/2 \sin \theta$).

N_2 adsorption isotherms of the adsorbents were measured at −196 °C on a Micromeritics ASAP 2010 sorptometer. Prior to measurement, all samples were outgassed at 110 °C at 10^{-6} mmHg. BET surface areas were measured from the linear part of the BET plot ($0.05 < P/P_0 < 0.25$). Mesopore volumes (V_{mp}) were assumed to be equal to the liquid volume of adsorbed nitrogen below $P/P_0 = 0.7$. Pore-size distributions were calculated using the Broekhoff−deBoer (BdB) method.[35]

Scanning electron microscopy (SEM) images of the adsorbents were obtained using a JEOL JSM6400 scanning electron microscope (Ontario Geosciences Laboratories).

Results and Discussion

All of the mesostructures in this study were prepared using a total silane/surfactant mole ratio of 8.0. Also, Igepal CA-720 was chosen as the assembly surfactant for all experiments. The choice of this particular surfactant was guided by its moderate cloud point temperature (measured at 75 °C), allowing the investigation of a vast synthesis temperature range (up to 71 °C) which approached the amphiphilic limit of the surfactant. The amount of fluoride used to catalyze the cross-linking of the silicate precursors was also kept rigorously constant (4.2 mol % with respect to total Si) in every preparation. Tables 1−4 summarize the structural properties of the MSU microspheres and that of their functional derivatives prepared under varying temperature and compositional conditions. Scanning electron micrographs of the materials confirmed that all samples possessed the uniform monodisperse microspherical morphology expected from the mild acid hydrolysis conditions used (Figure 1).[33−35]

Microsphere Framework and Pore Structure. The mesostructures prepared at lower synthesis tem-

(35) Bagshaw, S. A.; Prouzet, E.; Pinnavaia, T. J. *Science* **1995**, *269*, 1242.

Table 3. Structural Characteristics of MSU-2 Microspherical Mesostructures Prepared by Substituting 4.0 Mol % of TEOS with MPTMS

material designation	synthesis temp. (°C)	BET surface area ($m^2\ g^{-1}$)	mesopore volume ($cm^3\ g^{-1}$)	pore diameter (Å)	lattice spacing (Å)	wall thickness (Å)
MP-MSU-2(MS)-4.0-0	0	607	0.27	<20	34.5	>15
MP-MSU-2(MS)-4.0-10	10	378	0.16	<20	34.5	>15
MP-MSU-2(MS)-4.0-15	15	437	0.18	<20	36.4	>16
MP-MSU-2(MS)-4.0-20	20	464	0.20	<20	37.5	>18
MP-MSU-2(MS)-4.0-25	25	453	0.19	<20	37.8	>18
MP-MSU-2(MS)-4.0-30	30	652	0.29	<20	39.4	>19
MP-MSU-2(MS)-4.0-35	35	697	0.31	<20	40.2	>20
MP-MSU-2(MS)-4.0-40	40	706	0.31	<20	41.5	>22
MP-MSU-2(MS)-4.0-45	45	1571	0.90	30	44.3	14
MP-MSU-2(MS)-4.0-50	50	1259	0.84	32	45.9	14
MP-MSU-2(MS)-4.0-55	55	1198	0.78	34	47.5	14
MP-MSU-2(MS)-4.0-61	61	1146	0.97	38	48.1	10
MP-MSU-2(MS)-4.0-64	64	1041	0.98	41	50.6	10
MP-MSU-2(MS)-4.0-68	68	1059	0.95	41	50.0	9
MP-MSU-2(MS)-4.0-71	71	930	0.93	43	52.0	9

Table 4. Structural Characteristics of MSU-2 Microspherical Mesostructures Prepared by Substituting 6.0 Mol % of TEOS with MPTMS

material designation	synthesis temp. (°C)	BET surface area ($m^2\ g^{-1}$)	mesopore volume ($cm^3\ g^{-1}$)	pore diameter (Å)	lattice spacing (Å)	wall thickness (Å)
MP-MSU-2(MS)-6.0-0	0	628	0.29	<20	34.5	>15
MP-MSU-2(MS)-6.0-10	10	413	0.17	<20	33.6	>14
MP-MSU-2(MS)-6.0-15	15	454	0.20	<20	34.2	>14
MP-MSU-2(MS)-6.0-20	20	460	0.21	<20	39.0	>19
MP-MSU-2(MS)-6.0-25	25	613	0.27	<20	36.8	>17
MP-MSU-2(MS)-6.0-30	30	544	0.24	<20	38.2	>18
MP-MSU-2(MS)-6.0-35	35	850	0.39	<20	42.4	>22
MP-MSU-2(MS)-6.0-40	40	1182	0.65	29	44.8	16
MP-MSU-2(MS)-6.0-45	45	731	0.33	<20	39.8	>20
MP-MSU-2(MS)-6.0-50	50	741	0.32	<20	41.9	>22
MP-MSU-2(MS)-6.0-55	55	1246	0.77	30	46.4	16
MP-MSU-2(MS)-6.0-61	61	1154	0.84	32	48.0	16
MP-MSU-2(MS)-6.0-64	64	1093	0.97	36	49.3	13
MP-MSU-2(MS)-6.0-68	68	1143	0.94	37	48.1	11
MP-MSU-2(MS)-6.0-71	71	1050	0.94	43	50.0	7

peratures (below 40 °C) had rather low intensity, broad, and noisy X-ray diffraction patterns (Figure 2), especially below 25 °C. Compared to those of MSU-X mesostructures prepared at pH 7 under otherwise identical synthesis conditions, the XRD patterns were of uncharacteristically poor quality, and denoted very poor order in the mesostructure frameworks. The intensity of the peak, however, improved somewhat by increasing the synthesis temperature of the mesostructures (Figure 2), although the materials still had disappointingly poor order throughout the 0−40 °C range. Beginning from the temperature range 37−45 °C, however, a dramatic enhancement in the framework order of the materials was observed, as attested by the sudden enhancement of the XRD peak intensities at higher synthesis temperatures (Figure 3). In addition, the XRD signal maxima of the patterns shifted to lower diffraction angles upon increasing synthesis temperature (Figures 2 and 3), denoting a systematic increase in lattice spacing (Tables 1−4).

The N_2 isotherms of the mesostructures also exhibited striking differences in the synthesis temperature ranges before and after the 37−45 °C transition zone (Figure 4). Whereas the isotherms for all materials prepared at temperatures below the transition zone had type I appearance (viz, steep increase in adsorbed N_2 near $P/P_0 = 0$ followed by a sharp leveling off to constant adsorbed volume), those synthesized at temperatures above this range had type-IV appearance, with distinct inflections observed in the P/P_0 region between 0.2 and 0.5 (Figure 4). Pore size distributions calculated on the basis of these isotherms (Figure 5) confirmed that the former (i.e., pre-transition) mesostructures were microporous (pore diameters below 2 nm), whereas the latter (i.e., post-transition) were mesoporous (pore diameters of 3 nm and greater) and had average pore diameters which systematically increased as a function of increasing synthesis temperature (Figure 5, Tables 1−4).

Origin of Structural Transition. On the basis of the information presented in this work, a mechanism is proposed to explain the origin of the observed structural transition in the synthesis temperature range of 37−45 °C. This process is depicted in Scheme 1. Because the silane/surfactant mole ratios are constant throughout all of the experiments, and product formation was deemed to be quantitative in all of the preparations (100% yield), it follows that each of the synthesis mixtures will contain the same number of micelles and an identical amount of framework-forming silica precursors. The amphiphilic character of these micelles, however, changes as a function of the synthesis temperature, giving rise to mesostructures with pore diameters that increase as a function of increasing temperature.[30,32] Thus, at low synthesis temperatures

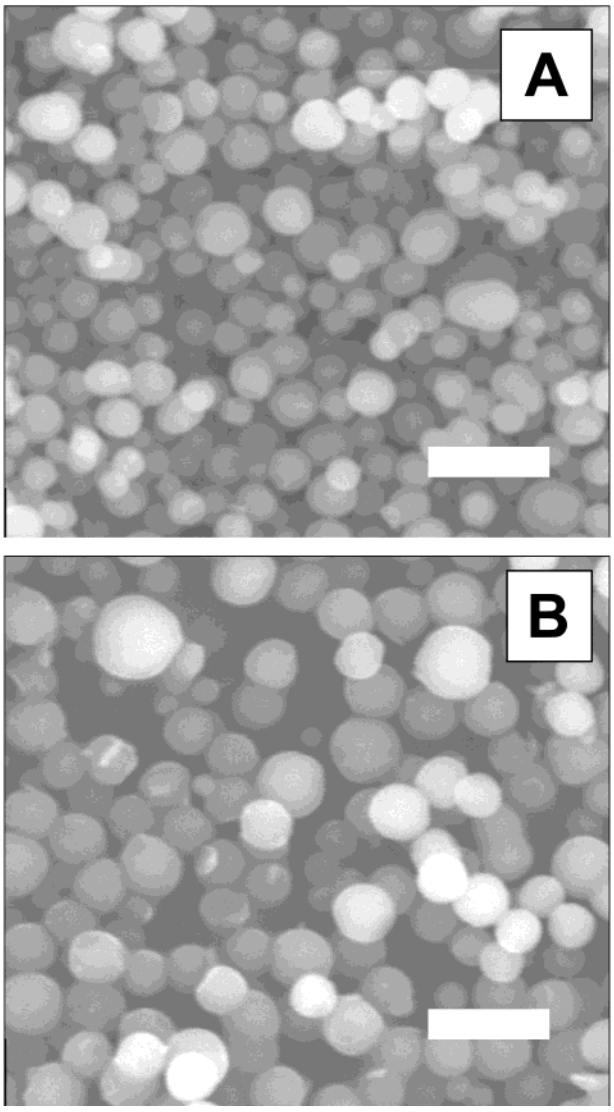

Figure 1. Scanning electron micrographs of representative MSU-2 microspheres prepared (a) at 25 °C and (b) at 40 °C. The white scale bars correspond to 10 μm.

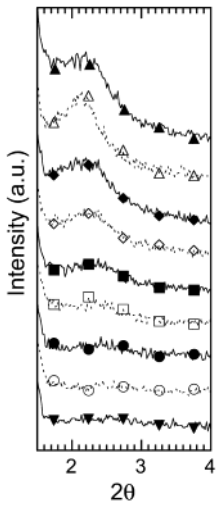

Figure 2. Powder XRD patterns for MP-MSU-4% microspheres prepared at (▼) 0 °C, (○) 10 °C, (●) 15 °C, (□) 20 °C, (■) 25 °C, (◇) 30 °C, (◆) 35 °C, (△) 37 °C, and (▲) 40 °C.

(lower than that of the transition range), the hydrophobic cores of the micelles are comparatively small and,

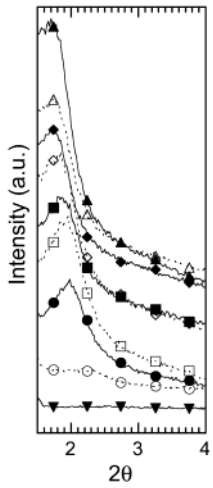

Figure 3. Powder XRD patterns for MP-MSU-4% microspheres prepared at (▼) 0 °C, (○) 40 °C, (●) 45 °C, (□) 50 °C, (■) 55 °C, (◇) 61 °C, (◆) 64 °C, (△) 68 °C, and (▲) 71 °C.

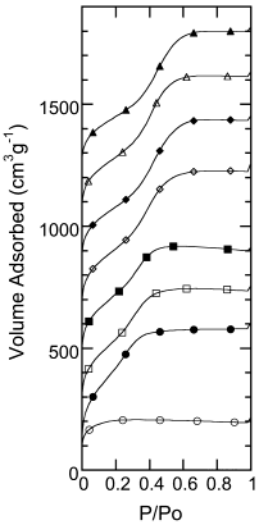

Figure 4. N_2 adsorption isotherms for MP-MSU-4% microspheres prepared at (○) 40 °C, (●) 45 °C, (□) 50 °C, (■) 55 °C, (◇) 61 °C, (◆) 64 °C, (△) 68 °C, and (▲) 71 °C. The isotherms of samples prepared at temperatures above 45 °C were offset by 200 cm^3g^{-1} for clarity.

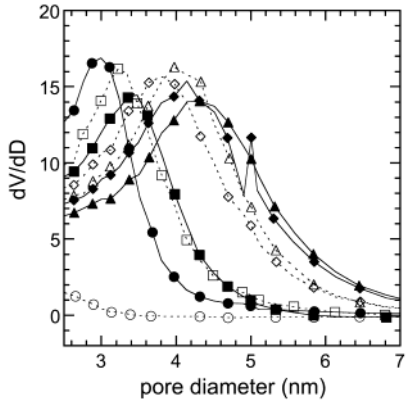

Figure 5. Pore-size distributions for MP-MSU-4% microspheres prepared at (○) 40 °C, (●) 45 °C, (□) 50 °C, (■) 55 °C, (◇) 61 °C, (◆) 64 °C, (△) 68 °C, and (▲) 71 °C.

conversely, the amphiphilic PEO corona is large. A recent report by Boissière et al. presented compelling evidence that the silica oligomers involved in MSU-X microsphere formation interacted with the PEO corona

Scheme 1. Representation of the Silicate Cross-Linking Process Involved in the Assembly of Nanoporous MSU Silica

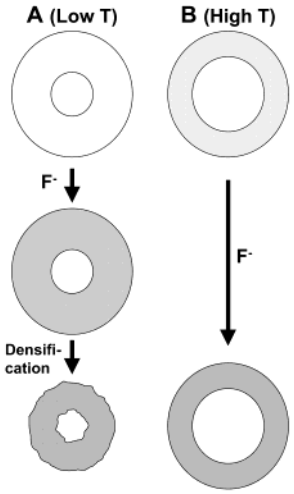

Pathway A, left, depicts the high dispersion of oligomeric silicate precursors in the amphiphilic PEO corona of the surfactant micelles at low synthesis temperature (top), that cross-link into a highly reticulated low-density silica framework upon fluoride addition (middle), which subsequently collapses into a more disordered microporous framework (bottom). Pathway B, right, depicts the more densely arranged silica precursors in the PEO corona of micelles at higher synthesis temperature (where the hydrophobic core is swollen, top), which forms a more highly cross-linked mesoporous framework (bottom) that does not undergo structural collapse.

prior to fluoride-induced cross-linking.[37] On the basis of this premise, it is proposed that the silica oligomers are highly dispersed in the voluminous PEO corona of the low-temperature micelles. When fluoride is added and cross-linking occurs, a highly reticulated silica network (with very low density) initially forms within the amphiphilic corona (Scheme 1, pathway A); a hypothesis which is supported by recently published evidence for MSU silicas.[38] This low-density gel precusor is likely too unstable to persist, and therefore subsequently collapses into a more densified silica framework (Scheme 1, pathway A). The densification process results in shrinkage of the pore diameter (to the micropore size range) and the lattice spacing. The structural collapse of the framework also results in perturbation of the framework order in the materials, giving rise to poor quality XRD patterns for these materials (Figure 2). As the synthesis temperature increases, the hydrophobic core of the micelle swells and the PEO corona correspondingly shrinks in size, resulting in a higher density of silicate oligomers in the PEO palissade. As a result, a more highly cross-linked gel (although still of very low density) forms upon fluoride addition. Although this gel precursor still collapses into a denser silica framework, the extent of this densification is less not as severe as that which occurred at lower temperature (viz, the precursor gel is already of greater density), forming a mesostructure with correspondingly higher lattice spacings, pore diameters, and improved framework order.

(36) Broekhoff, J. C. P.; de Boer, J. H. *J. Catal.* **1968**, *10*, 377.
(37) Boissière, C.; Larbot, A.; Bourgaux, C.; Prouzet, E.; Bunton, C. A. *Chem. Mater.* **2001**, *13*, 3580.
(38) Bagshaw, S. A. *Chem. Commun.* **1999**, 271.

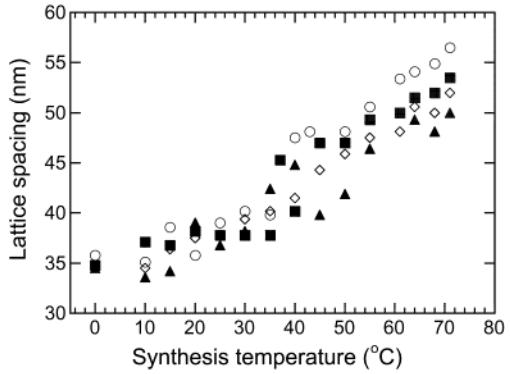

Figure 6. Effect of temperature on lattice spacings of (○) pristine MSU-2, (■) MP-MSU-2%, (◇) MP-MSU-4%, and (▲) MP-MSU-6% microspheres.

When the 37−40 °C temperature range is reached, the receding front of the amphiphilic PEO corona continues to diminish the latter's volume. At this stage, the density of silica oligomers inside the corona reaches a point where they can cross-link upon fluoride addition to form silica frameworks which are sufficiently stable so as to not undergo further densification (Scheme 1, pathway B). The resulting silica frameworks thus retain the original shape bestowed to them by the assembling surfactant micelles, and mesostructured materials with greatly improved framework order are obtained. It is noteworthy to mention that the *d* spacings and pore sizes of mesostructures prepared at synthesis temperatures beyond 40 °C are similar to those of mesostructures prepared at similar temperatures using the neutral pH assembly method.[30] From that point on, further increases in synthesis temperatures results in materials with progressively increased *d* spacings, pore diameters, and volumes (Tables 1−4). The XRD peaks, moreover, are also found to become more intense for materials prepared at higher synthesis temperatures (Figure 3), while their apparent wall thicknesses decrease (Tables 1−4). As the PEO corona continues to be "thinned out" as the hydrophobic micelle core swells under the influence of temperature, the silica oligomers become increasingly packed together, resulting in framework walls which are thinner, yet composed of an increasingly dense silica framework. The continuing densification of the framework thus results in the progressive improvement of structural order in the mesostructures.

Influence of Synthesis Parameters on Nanostructural Properties. Figures 6, 7, and 8 show the temperature-dependent evolution of the mesostructures' lattice spacings, mesopore volumes, and mesopore diameters, respectively. Different trends in the progession of these properties are generally observed before and after the structural transition temperature (37−45 °C) range. For instance, the *d* spacings are found to increase more steeply as a function of synthesis temperature beyond the transition point (Figure 6). The pore volumes also sharply increase in size beyond the 37−45 °C temperature range (Figure 7). These observations demonstrate once again the sharp contrast in material properties resulting from the modification of synthesis temperature, as previously discussed. By simultaneously varying the synthesis temperature and the organosilane content, judicious control over the pore

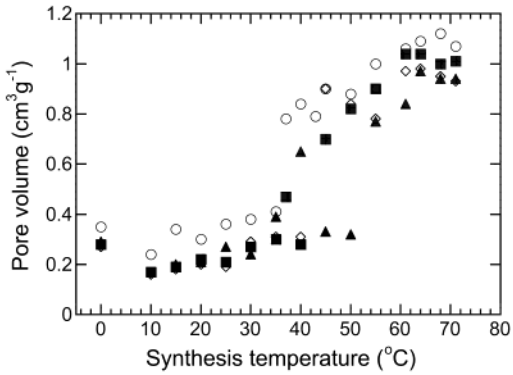

Figure 7. Effect of temperature on pore volumes of (○) pristine MSU-2, (■) MP-MSU-2%, (◇) MP-MSU-4%, and (△) MP-MSU-6% microspheres.

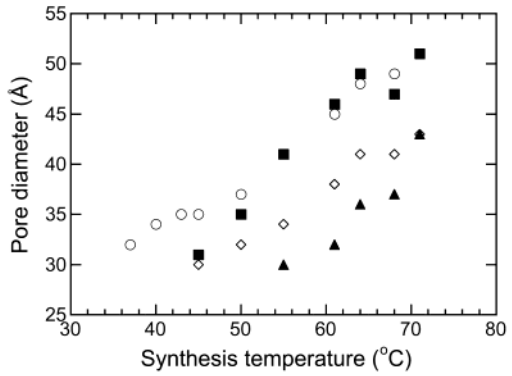

Figure 8. Effect of temperature on pore diameters of (○) pristine MSU-2, (■) MP-MSU-2%, (◇) MP-MSU-4%, and (▲) MP-MSU-6% microspheres.

diameters of the microspheres can be achieved (Figure 8).

The degree of organosilane (mercaptopropyl) loading inside the mesostructures also manifests an influence on their nanostructure. The presence of a higher loading on organic moieties results in the systematic reduction of pore volume and pore diameter expected from the presence of increasing amounts of organic functions inside the nanopore channels (Figures 6−8). A slight decrease in the lattice spacing of the materials is also observed in materials with increasing organosilane content (Figure 6). Richer and Mercier recently reported a similar effect in organically functionalized MSU silicas prepared under neutral pH assembly conditions,[30] but the lattice contraction effect observed in the present work was much less dramatic than that observed by these authors. Under neutral pH conditions, TEOS and MPTMS do not undergo rapid hydrolysis and therefore dissolve directly into the micelles' PEO corona and core.[30] This creates a partition of the TEOS and MPTMS precursors inside the micelles, wherein the more hydrophobic MPTMS molecules penetrate deeper inside the micelles' hydrophobic core.[30] This subsequently results in mesostructures with pore sizes that are significantly smaller than those obtained when only TEOS is used (an effect which was particularly evident at high synthesis temperatures).[30] On the other hand, the acidic conditions used to prepare the microspherical MSU mesostructures in the present work result in the hydrolysis of TEOS and MPTMS prior to mesostructure formation. The oligomeric precursors thus formed are much more water soluble than their parent alkoxysilanes and therefore do not penetrate inside the hydrophobic core of the micelles, but rather remain exclusively within in the amphiphilic PEO corona of the surfactant mesophase.[37] As a result, the influence of the hydrophobic organic chains on MPTMS occluded within these oligomers is dramatically reduced, although not altogether eliminated because the presence of organic moieties on the silica oligomers will favor their retention towards the hydrophobic core of the micelles. The hydrophobic retention of these "organosilica" oligomers can also be invoked to explain the observed shift in the structural transition temperature in the mesostructures containing higher loading of mercaptopropyl groups (i.e., from about 37 °C for pristine MSU-2 to about 45 °C for MP-MSU-6%; Figures 6 and 7).

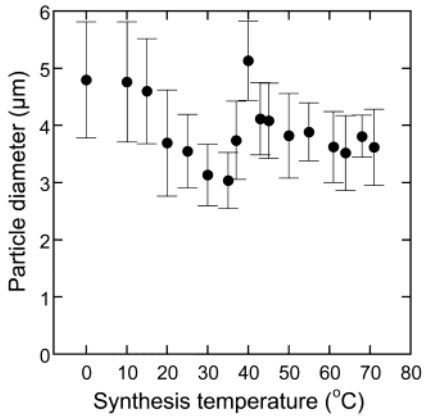

Figure 9. Average particle sizes of MSU silica microspheres prepared at various synthesis temperatures. The error bars represent the standard deviations of particle diameters within each representative sample.

Influence of Synthesis Temperature on Particle Morphology. Detailed microsphere size distributions were determined from the SEM micrographs of MSU-2 silicas prepared at different synthesis temperatures (Figure 9). In the temperature range from 0 to 35 °C, the MSU microspheres were found to systematically diminish in size. Moreover, the time required for product formation was found to decrease as a function of increasing synthesis temperature, which suggests that the rate of nucleation of the microspheres becomes more significant compared to the rate of particle growth at higher temperature, giving rise to the observed trend. At the 37−45 °C temperature range, however, a sudden jump in particle size is observed. This jump is associated with the previously discussed structural transition that the microspheres undergo in the same temperature range, and can be explained by the sudden expansion of the framework lattice of the materials resulting from the structural transition. Beyond the transition temperature range, the particle sizes resume their decreasing trend as nucleation rates continue to increase with temperature. These observations demonstrate that synthesis temperature can be used not only to control the nanostructural properties of the mesostructures (lattice spacings, pore sizes), but also constitutes a means of achieving control over the particle size of MSU-X mesostructures.

Influence of Organic Functional Group on Mesostructure Properties. Preliminary experiments have

shown that the mild acid synthesis of similar types of functional MSU mesostructures can be obtained from a wide variety of functional groups other than mercaptopropyl. Thus, nanoporous silica microspheres into which octyl, propyl, and phenyl moieties are incorporated can be prepared, demonstrating the generality of the synthesis method. Further discussion, however, on the influence of diverse organic functional groups is not within the scope of the current report, and will be presented in greater detail in an upcoming article.

Conclusion

This work has explored the effect of various synthesis parameters (including temperature and organic group loading) on the structure and morphology of mercaptopropyl-functionalized nanoporous silica microspheres. Synthesis temperature was found to be an especially crucial determinant of the framework structure, pore dimension, and particle size for these materials. By demonstrating the ability to control both nanoscale and microscale properties of nanostructured materials, these findings will be useful for the design of new functional materials with tailored functionality, pore structure, and morphology (i.e., adsorbents, catalysts, chromatographic supports, etc.).

Acknowledgment. We thank the Natural Science and Engineering Research Council of Canada (NSERC) for financial support. We also thank L. Semenyna (Ontario Geosciences Laboratory) for providing technical support with SEM.

CM021294L